 doi:10.1111/j.1462-5822.2005.00551.x

PilT is required for PI(3,4,5)P3-mediated crosstalk between *Neisseria gonorrhoeae* and epithelial cells

Shaun W. Lee,[1†] Dustin L. Higashi,[1] Aurelie Snyder,[1] Alexey J. Merz,[1‡] Laura Potter[1§] and Magdalene So[1]*
Department of Molecular Microbiology and Immunology, L220, Oregon Health and Science University, Portland, OR 97239-3098, USA.

Summary

The retractile type IV pilus participates in a number of fundamental bacterial processes, including motility, DNA transformation, fruiting body formation and attachment to host cells. Retraction of the *N. gonorrhoeae* type IV pilus requires a functional *pilT*. Retraction generates substantial force on its substrate (> 100 pN per retraction event), and it has been speculated that epithelial cells sense and respond to these forces during infection. We provide evidence that piliated, Opa non-expressing *Neisseria gonorrhoeae* activates the stress-responsive PI-3 kinase/Akt (PKB) pathway in human epithelial cells, and activation is enhanced by a functional *pilT*. PI-3 kinase inhibitors wortmannin and LY294002 reduce cell entry by 81% and 50%, respectively, illustrating the importance of this cascade in bacterial invasion. PI-3 kinase and its direct downstream effectors [PI(3,4,5)P3] and Akt are concentrated in the cell cortex beneath adherent bacteria, particularly at the periphery of the bacterial microcolonies. Furthermore, [PI(3,4,5)P3] is translocated to the outer leaflet of the plasma membrane. Finally, we show that [PI(3,4,5)P3] stimulates microcolony formation and upregulates *pilT* expression *in vitro*. We conclude that *N. gonorrhoeae* activation of PI-3 kinase triggers the host cell to produce a lipid second messenger that influences bacterial behaviour.

Introduction

Type IV pili are produced by a wide variety of bacteria, including *Myxococcus xanthus*, *Synechocystis* spp., *Vibrio cholerae*, enteropathogenic and enterohaemorrhagic *Escherichia coli, Pseudomonas aeruginosa, Neisseria gonorrhoeae* (GC) *and Neisseria meningitidis* (see review, Strom and Lory, 1993). These structures play important roles in motility-associated behaviour such as fruiting body and biofilm formation, phototaxis, phage sensitivity and virulence (Wu *et al*., 1997; Comolli *et al*., 1999; Merz and So, 2000a; Bhaya *et al*., 2001).

The GC type IV pilus binds human complement regulatory protein CD46 in some cell types (Kallstrom *et al*., 1997). Piliated bacteria trigger tyrosine phosphorylation of the CD46 cytosolic tail 2 isoform in A431 epidermoid carcinoma cells (Lee *et al*., 2002). They induce the release of free Ca^{2+} from intracellular stores, which redirects trafficking of Lamp1 compartments and promotes bacterial intracellular survival (Kallstrom *et al*., 1997; Lin *et al*., 1997; Ayala *et al*., 2001). These activities of the GC type IV pilus strongly suggest that the structure modulates host cell signalling cascades that influence infectivity.

Type IV pili are retractile structures (Merz *et al*., 2000b; Skerker and Berg, 2001). Retraction of a single GC pilus often generates forces greater than 100 pN (Merz *et al*., 2000b; Maier *et al*., 2002). Retraction requires PilT, a member of a large family of putative NTPases from type II and type IV secretion systems (Wolfgang *et al*., 1998a,b; Herdendorf *et al*., 2002). GC *pilT* null mutants are piliated but cannot retract pili (Merz *et al*., 2000b). They are non-motile (Wolfgang *et al*., 1998b). They aggregate into microcolonies, though these structures have an aberrant appearance. They adhere to epithelial cells, but are unable to trigger the formation of cortical plaques – structures in the host cell cortex beneath adherent bacteria containing high concentrations of cytoskeletal components, transmembrane receptors and other signalling proteins (Merz *et al*., 1999). Finally, *pilT* mutants cannot be transformed with DNA (Wolfgang *et al*., 1998b).

How pilus retraction might influence infectivity is unknown. Mechanical forces less than 80 pN exerted on the plasma membrane of mammalian cells trigger Ca^{2+} fluxes and induce signalling cascades, promoting, among other events, cytoskeleton reorganization during cell–cell and cell–substrate adhesion and cellular adhesion plaque formation (Wang *et al*., 1993; Raucher *et al*., 2000; Berridge *et al*., 2003). Pilus retraction during bacterial attachment may therefore generate sufficient force on the

Received 7 March, 2005; revised 8 April, 2005; accepted 12 April, 2005. *For correspondence. E-mail somaggie@ohsu.edu; Tel. (+1) 503 494 7768; Fax (+1) 503 494 6862.Present addresses: †Department of Pharmacology, University of California, San Diego, La Jolla, CA 92093-0721, USA; ‡Department of Biochemistry, University of Washington, Seattle, WA 98195, USA; §Leicester Warwick Medical Schools, University of Warwick, Gibbet Hill campus, Coventry, CV4 7AL, UK.

epithelial membrane to trigger cellular signals that influence the course of infection.

One signal cascade that is activated through membrane tension is the phosphoinositide-3 (PI-3) kinase pathway (Miao *et al*., 2002). PI-3 kinases orchestrate many cellular events, including cell growth, motility, differentiation, survival and trafficking (Cantley, 2002). PI-3 kinases have been implicated in bacterial virulence. Efficient entry into host cells by *Listeria monocytogenes*, *Helicobacter pylori* and *Chlamydia pneumoniae* require activated PI-3 kinase (Ireton and Cossart, 1997; Coombes *et al*., 2002; Kwok *et al*., 2002). Invasion of Opa-expressing, non-piliated GC through the CEACAM-3 receptor is also stimulated by PI-3 kinase (Booth *et al*., 2003).

We tested the hypothesis that pilus retraction activates the PI-3 kinase pathway. We report that GC infection activates the PI-3 kinase/Akt pathway in a process that involves *pilT*. The cascade triggers the epithelial cell to produce a lipid second messenger that, in turn, affects bacterial motility behaviour.

Results

PI-3 kinase and Akt are activated upon GC infection

We tested the hypothesis that pilus retraction during infection activates PI-3 kinase, as this pathway is known to be activated by membrane tension. Akt activity served as the indicator of PI-3 kinase activation, as Akt is a direct downstream effector of PI-3 kinase. A431 cells were infected for various lengths of time with wild-type (wt) GC strain MS11 or MS11*pilT*, a piliated, Opa non-expressing strain with a null mutation in *pilT*. This mutant adheres normally to cells, forms microcolonies, but fails to retract pili. Akt was immunoprecipitated from cell lysates and tested for its ability to phosphorylate the Akt substrate GSK-3α/β. Phospho-GSK-3α/β levels rose within 30 min after infection with wt MS11, suggesting Akt activation, and the levels remained high for 3 h (Fig. 1A; upper panel). In contrast, phospho-GSK-3α/β levels were significantly lower in cells infected with the *pilT* null mutant (Fig. 1B; upper panel). Control immunoblots of total cell lysates

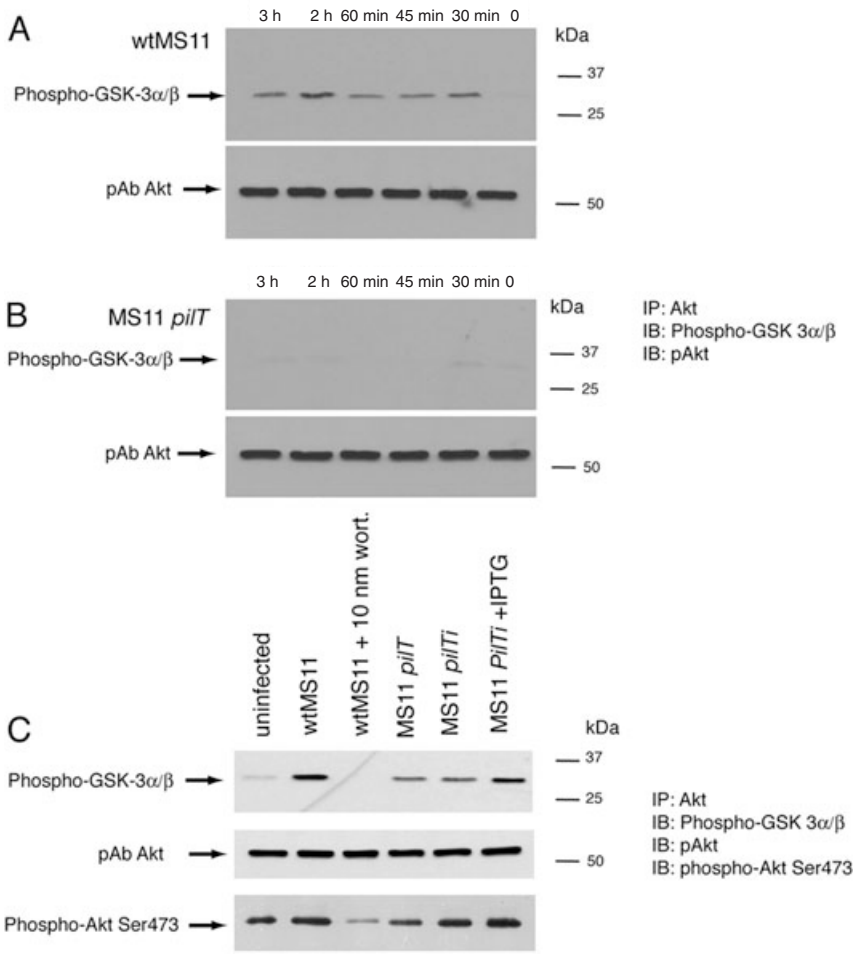

Fig. 1. Activity of Akt in GC-infected cells. A431 cells were infected for various lengths of time with wt MS11 (A) or MS11*pilT* (B), and Akt was immunoprecipitated from the lysates and assayed for its ability to phosphorylate GSK-3αβ *in vitro*. Phospho-GSK-3α/β was detected by immunoblotting using a phospho-GSK-3α/β antibody (top panels). Total Akt levels in input lysates were detected by immunoblotting using an antibody to phosphorylated and unphosphorylated Akt (bottom panels). A431 cells were infected for 30 min with wt or *pilT* mutants of MS11, in the presence of wortmannin (wort) or IPTG (C). Akt activity in the precipitates (top panel) and total Akt levels in input lysates (middle panel) were detected as above. Activated Akt levels in total lysates were detected by immunoblotting using an antibody to Akt phosphorylated at Ser473 (bottom panel).

using an anti-Akt antibody showed that equal amounts of Akt were present in the samples (Fig. 1A and B, lower panels).

The influence of pilus retraction on Akt activation was further examined using MS11*placZ-pilT*, a strain in which *pilT* is under control of an IPTG-inducible promoter. A431 cells were infected for 30 min with wt MS11, MS11*pilT*, or MS11*placZ-pilT*, and Akt activity was assessed as described above. Like the previous experiment, phospho-GSK-3α/β levels were higher in cells infected with wt MS11 than in cells infected with either *pilT* mutant (Fig. 1C, upper panel). However, phospho-GSK-3α/β levels noticeably rose when IPTG was added to the cultures infected with MS11*placZ-pilT*. Immunoblots of the input, total cell lysates using an antibody recognizing phosphorylated and unphosphorylated Akt showed that variations in Akt activity were not resulting from loading error (middle panel). Additional immunoblots of input lysates with an anti-phospho-Akt Ser473 antibody showed that the appearance of phospho-Akt coincided with Akt activity on GSK-3α/β, confirming Akt activation in infected cells (lower panel).

The difference in intensity of the phospho-GSK-3α/β bands in Fig. 1B and C is a result of differences in exposure times of the immunoblots. Longer exposures of the blot shown in Fig. 1B revealed phospho-GSK-3α/β bands in infected cell lysates, these bands being more intense that those in the uninfected (0 h) lane (data not shown).

Finally, the PI-3 kinase inhibitor wortmannin blocked Akt activation in MS11-infected cells, verifying the dependence of Akt activation on PI-3 kinase (Fig. 1C, upper panel). Control experiments indicated that wortmannin did not affect bacterial viability or growth (data not shown).

Thus, infection of epithelial cells with piliated, Opa non-expressing GC activates the PI-3 kinase/Akt pathway in a process that is influenced by *pilT*.

Invasion of piliated GC is partially dependent on PI-3 kinase activation

PI-3 kinase contributes to cell invasion by several bacterial pathogens (Ireton and Cossart, 1997; Coombes *et al*., 2002; Kwok *et al*., 2002). We therefore determined whether the PI-3 kinase pathway also influenced GC cell entry. A431 cells were infected with wt MS11 for 6 h in the presence or absence of PI-3 kinase inhibitors wortmannin or LY294002. The bacterial invasion index was determined using the Gentamicin protection assay (Shaw and Falkow, 1988; Makino *et al*., 1991; Gomez-Duarte *et al*., 1997). This assay allows quantification of intracellular, or Gentamicin-protected, bacteria on a large scale. Each infection was performed in triplicate, and each experiment was repeated three times with similar results. Wortmannin and LY294002 reduced MS11 invasion by 81.6% ($P = 0.005$) and 50% ($P = 0.001$) respectively (Fig. 2A and B). The inhibitors did not affect bacterial viability, growth, or adhesion to cells (data not shown). These results suggest that entry of piliated, Opa non-expressing GC into epithelial cells requires, in part, the PI-3 kinase pathway.

We next determined whether GC invasion via the PI-3 kinase pathway requires a functional *pilT*. The invasion index of wt MS11 and MS11*pilT* was compared. MS11*pilT* adhered to A431 cells like the wt parent strain (data not shown). However, its invasiveness was reduced by 40% ($P = 0.040$; Fig. 2C). The same *pilT* mutation in another genetic background resulted in an identical invasion defect (data not shown). Although invasion was significantly reduced in the *pilT* mutant, it was not completely abolished. Thus, GC enters cells through *pilT* dependent and independent pathways.

Finally, we assessed the role of PI-3 kinase in cell entry. The invasion index of the MS11*pilT* mutant was determined in the presence or absence of PI-3 kinase inhibitor LY294002 (Fig. 2D). LY294002 did not affect the ability of MS11*pilT* to enter cells. Thus, PI-3 kinase is only involved in the *pilT*-dependent invasion pathway.

PI-3 kinase and its downstream effectors cluster at the base of microcolonies

Piliated *Neisseria* trigger the formation of cortical plaques in infected cells directly beneath sites of bacterial attachment. These structures, visible for 3–4 h after infection, are enriched in membrane and other signalling proteins and cytoskeletal components (Merz *et al*., 1999; Hoffmann *et al*., 2001a). We next determined the location of PI-3 kinase and Akt in infected cells. Cells were infected for 3 h with wt MS11 and processed for immunofluorescence microscopy using antibodies recognizing the PI-3 kinase p110 catalytic subunit, phospho-Akt Ser473, or ezrin, a cytoskeleton component present in Neisseria-induced cortical plaques. Fluorescence was absent in control experiments using primary or secondary antibodies alone (data not shown).

Successive 0.1 μm thick vertical (Z)-sections of infected cells from the apical to the basolateral membrane revealed high concentrations of PI-3 kinase, phospho-Akt and ezrin at the cell cortex, particularly at the periphery of the microcolonies (Fig. 3A–F). Image overlays demonstrated the colocalization of PI-3 kinase and Akt with ezrin. Three-dimensional reconstructions of the same stack of Z-section images supported this interpretation. Ezrin concentrated beneath the microcolony. They also clustered within the microvilli at this site (Fig. 3G–I), giving the cell surface a brush-like appearance. In contrast, neither PI-3 kinase nor phospho-Akt clustered beneath adherent MS11*pilT* (Fig. 4A). Thus, GC clusters PI-3 kinase p110 and phospho-Akt at sites of infection, and this process involves *pilT*.

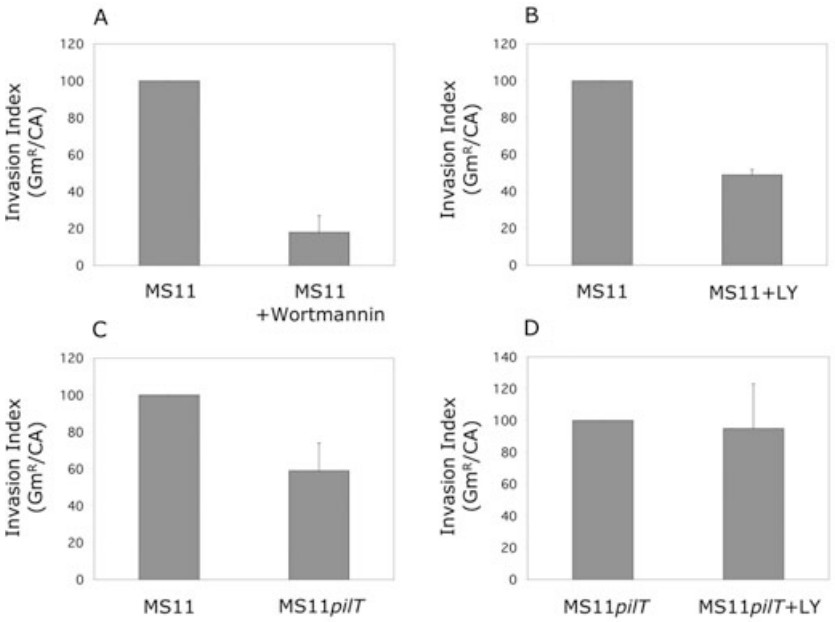

Fig. 2. Inhibition of GC invasion by PI-3 kinase inhibitors. A431 cells were infected with wt MS11 in the presence or absence of PI-3 kinase inhibitor, and the invasion index of the strain was scored (see *Experimental procedures*).
A. Invasion index of wt MS11 in the presence of 10 nM wortmannin (wort) and (B) 50 μM LY294002.
C. Invasion indices of wt MS11 and MS11*pilT* without inhibitor.
D. Invasion index of MS11*pilT* in the presence of 50 μM LY294002. Gm^R: Gentamicin resistant colony forming units; CA: cell-associated colony forming units. Experiments are referenced against a normalized control with an assigned value of 100%. Error bars indicate mean + SD derived from triplicate determinations from one representative experiment. Three independent experiments were performed for each treatment, with similar results.

[PI(3,4,5)P3] is translocated to the outer leaflet of infected cell membranes

Activated PI-3 kinase phosphorylates [PI(4,5)P2], generating [PI(3,4,5)P3]. This lipid second messenger recruits Akt to the membrane, leading to its subsequent activation. The clustering of activated PI-3 kinase and Akt at sites of GC attachment predicts that these sites will also have high levels of [PI(3,4,5)P3]. Immunofluorescence microscopy of MS11-infected cells using anti-[PI(3,4,5)P3] antibodies revealed accumulations of this phospholipid around microcolonies (Fig. 4B).

Infected unpermeabilized cells were also stained with the [PI(3,4,5)P3] antibody (Fig. 4B). In these experiments, saponin was omitted from the fixation protocol and all processing steps were performed at 4°C to minimize antibody entry. Under the same conditions, infected cells did not stain with an antibody to PARP, a cytosolic protein (Fig. 4B). This differential staining of [PI(3,4,5)P3] suggests that the phospholipid is surface exposed. In contrast, [PI(3,4,5)P3] did not cluster nor become surface exposed when cells were infected with the MS11*pilT* mutant (data not shown). Thus, GC clusters [PI(3,4,5)P3] in a pattern resembling PI-3 kinase p110 and phospho-Akt at sites of infection, and this process involves *pilT*.

A number of pathogens trigger rapid externalization of phosphatidylserine (PS) in infected cells (Fujimoto *et al*., 1998; Gao and Abu Kwaik, 1999; Goth and Stephens, 2001; Yilmaz *et al*., 2004). PS is normally sequestered on the cytosolic face of the plasma membrane, but can be rapidly and transiently translocated to the outer leaflet of the membrane. Infected cells were stained with a monoclonal antibody to PS (Chemicon) to examine membrane translocation of this lipid species during the course of infection. Some PS externalized to the outer membrane of A431 cells upon infection by MS11 (Fig. 4C, upper panel). In contrast to [PI(3,4,5)P3], externalized PS did not cluster around adherent bacteria. In non-permeabilized cells, costaining with the known plaque component phosphoERM(ezrin-radixin-moesin) was absent, confirming the specific staining of outer membrane species in our immunofluorescence assays (Fig. 4C, upper panel). This experiment was repeated with the addition of the membrane permeabilizing agent saponin (Fig. 4C, lower panel). Under these conditions, phosphoERM is shown clustering beneath adherent microcolonies. Furthermore, staining of PS in the nucleus after permeabilization was pronounced. Taken together, these data support the finding that lipid translocation takes place upon infection by wt GC expressing a functional PilT protein. Furthermore, [PI(3,4,5)P3], but not PS, translocates to areas directly beneath microcolony formation, implying that the lipid externalization by GC infection is specific for [PI(3,4,5)P3] and is not a general phenomenon of lipid membrane depolarization.

A marker of PS translocation is the phosphorylation of α-adducin at Ser 724 in host cells (Chapline *et al*., 1993; Dong *et al*., 1995). To lend further support for lipid translocation, infected cells were assayed for the presence of phospho-adducin.

A431 cells were infected for various lengths of time with MS11 or MS11*pilT* and the lysates were probed for phospho-adducin at Ser 724. Phospho-adducin levels were noticeably increased after 2 h of infection with MS11 or TPA treatment (Fig. 4D). This lends additional support to the observation that lipid translocation occurs in infected

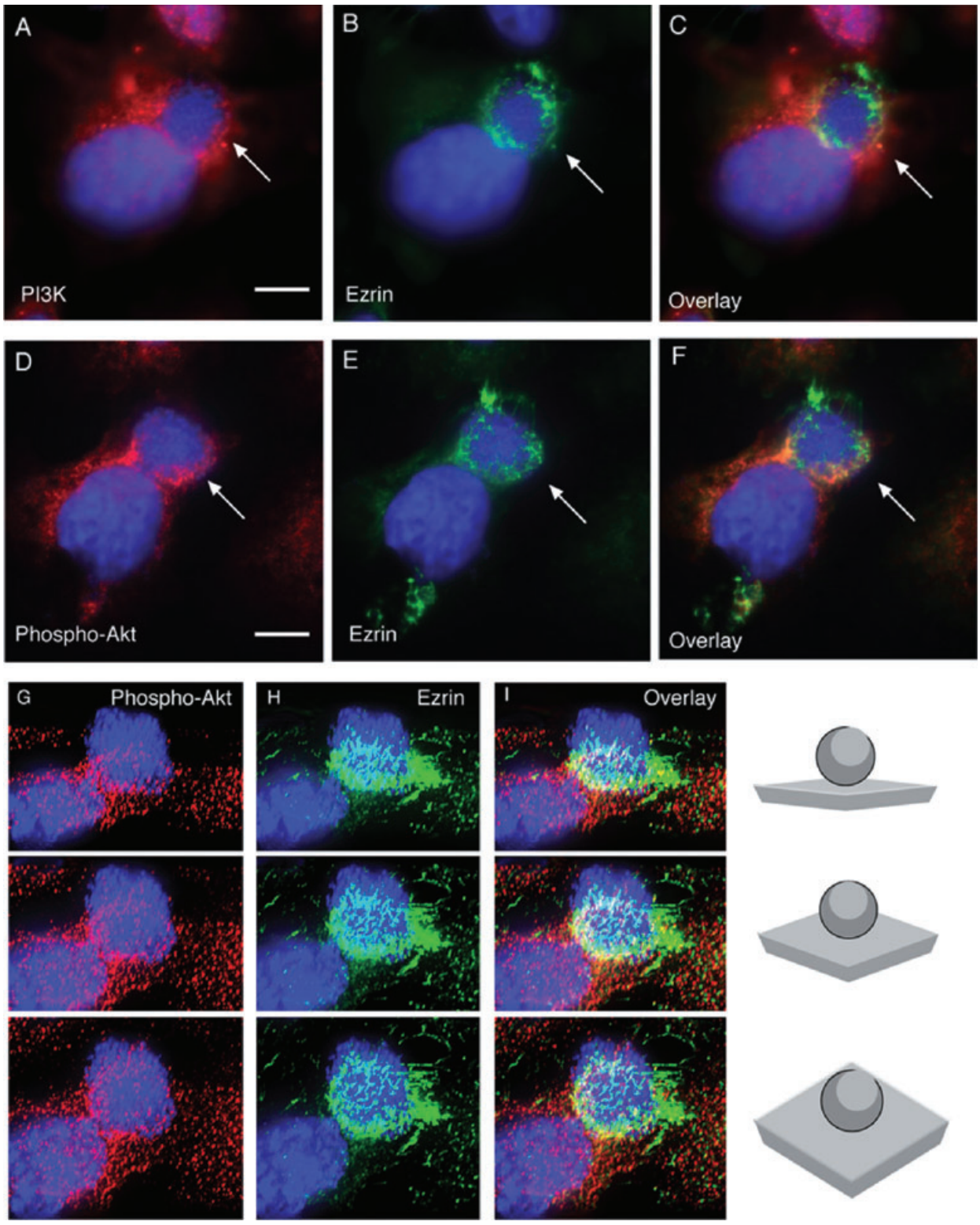

Fig. 3. PI3K p110 and phospho-Akt clustering in GC-infected cells. A431 cells were infected with wt MS11 for 3 h, then fixed and processed for indirect immunofluorescence microscopy using antibodies against PI-3 kinase p110 (A), ezrin (B), or phospho-Akt (D). The image shown in C and F are superimposed images shown in A and B, and D and E respectively. Arrows indicate location of microcolonies. Scale bar: 10 μM. Three-dimensional reconstructions of phospho-Akt and ezrin images shown in D, E and F. The reconstructed images in each column are the same; they have been rotated from the horizontal plane by advancing degrees (see cartoon on the right) to further illustrate the structures of the protein clusters. Images were deconvolved and the Volume Builder algorithm was performed using Deltavision Softworx software.

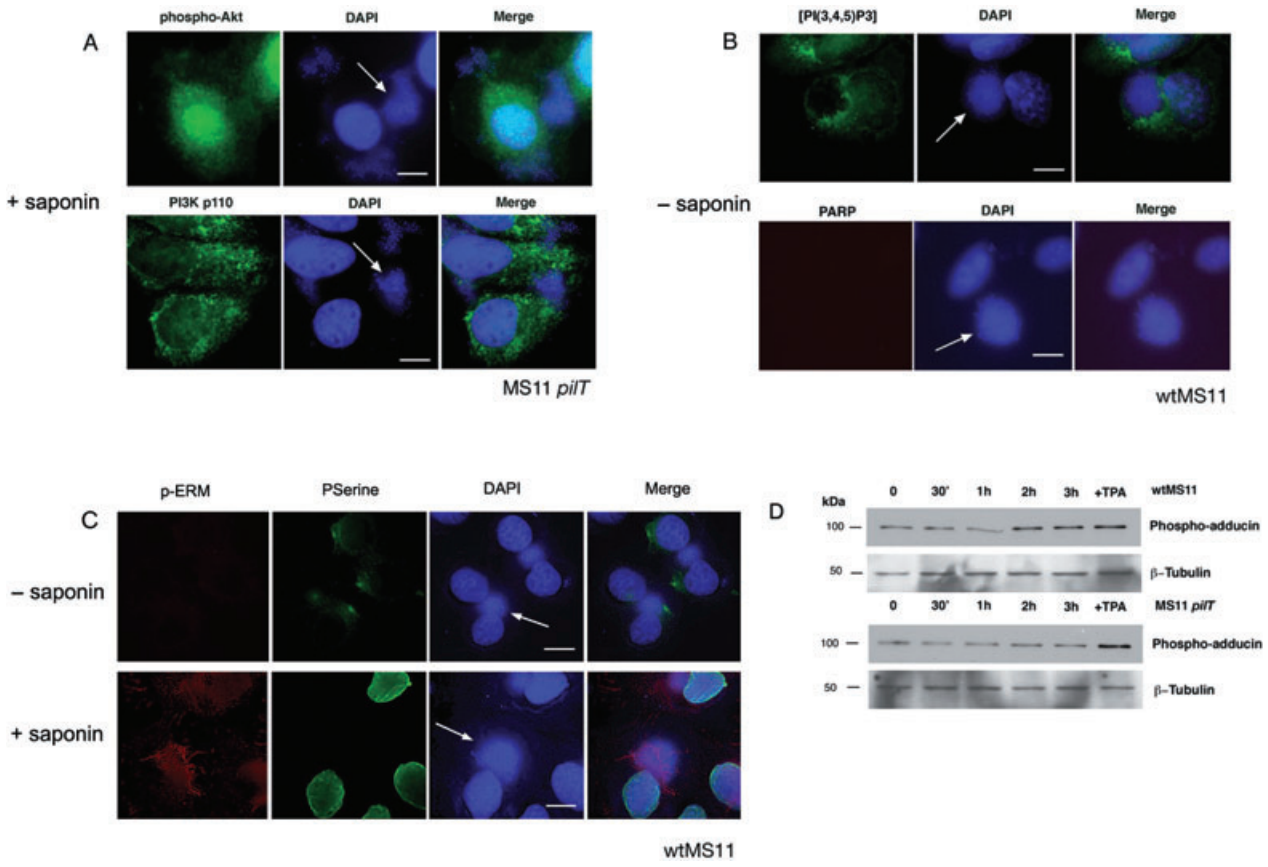

Fig. 4. Clustering of PI-3 kinase, phospho-Akt and [PI(3,4,5)P3] in GC-infected cells. A431 cells were infected with MS11*pilT* (A) or wt MS11 (B, C) for 3 h, and the cells were fixed and stained for indirect immunofluorescence microscopy using antibodies specific to phospho-Akt, PI-3 kinase, [PI(3,4,5)P3], PARP, or phosphatidylserine (green). DNA from bacteria and nuclei were stained with DAPI (blue). Images were acquired from cells treated with or without the membrane-permeabilizing detergent saponin prior to incubation with primary antibody. (To avoid membrane permeabilization and antibody entry into cells, saponin was excluded from the fixation process and all incubations were performed at 4°C). Staining is as follows:
A. PhosphoAkt, upper panel; PI3Kp110, lower panel.
B. [PI(3,4,5)P3], upper panel; PARP, lower panel.
C. Phospho-ERM, red; phosphadtidylserine, green. Merge: superimposed images from the left panels of the same row. Arrows indicate location of microcolonies. Scale bar: 10 μM.
D. Detection of phosphorylated adducin in A431 cells infected with wt MS11 or MS11*pilT* by immunoblotting with a phospho-adducin antibody. TPA induction of phospho-adducin in uninfected cells treated for 1 h with Phorbol-12 Myristate-13–Acetate (0.2 μM). In each experiment, input samples were probed with antibodies to β-tubulin as a loading control (bottom panels).

cell membranes, and is in direct support of our immunofluorescence data. Phospho-adducin levels were unchanged in MS11*pilT*-infected cells, strongly suggesting that *pilT* is required for lipid translocation. Reprobing of the same blots with an anti-β-tubulin antibody showed equal sample loading (Fig. 4D, lower panels).

We also determined whether infected cells released [PI(3,4,5)P3] into the medium. ELISA was used to determine total [PI(3,4,5)P3] concentrations in infected and uninfected cell supernates. In numerous assays, nearly identical amounts of [PI(3,4,5)P3] were detected in supernates of infected and uninfected cells (26.4 ± 1.7 SD pmol). Thus, [PI(3,4,5)P3] is anchored to the infected cell membrane and not released into the medium.

[PI(3,4,5)P3] modulates bacterial behaviour

The proximity of [PI(3,4,5)P3] to adherent GC led us to determine whether this phospholipid affected bacterial behaviour, in particular, microcolony formation and twitching motility. An aggregation assay was first performed. Wild-type MS11 cells were incubated for 1 h with 10 μg of [PI(3,4,5)P3] or vehicle alone, and microcolony formation was assessed by live-cell imaging and Differential Interference Contrast microscopy. Bacteria incubated with [PI(3,4,5)P3] or vehicle were motile. However, bacteria exposed to [PI(3,4,5)P3] aggregated into microcolonies more quickly than those in the presence of vehicle (Fig. 5). Moreover, microcolonies formed in the presence of the

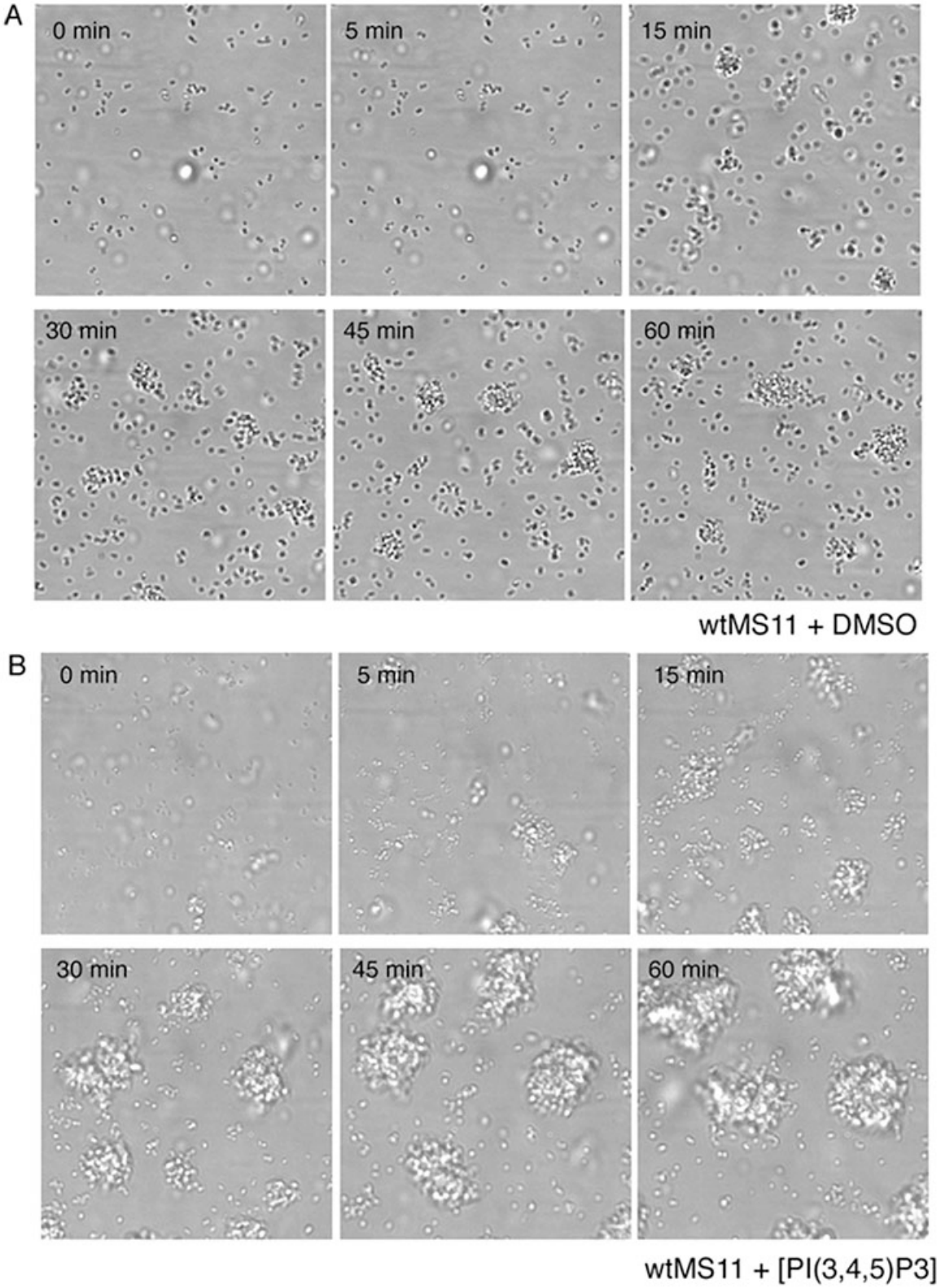

Fig. 5. Microcolony formation in the presence of soluble [PI(3,4,5)P3]. MS11 bacteria were suspended on a glass slide and incubated for 60 min with vehicle (A) or soluble PI(3,4,5)P3 (B) and microcolony formation was visualized by Differential Interference Contrast time-lapsed microscopy. Both sets of images were acquired at the same magnification.

lipid were much larger than those formed in the presence of the vehicle. As an additional control, bacteria were exposed to the lipid species [PI(4,5)P2] under identical conditions. Interestingly, bacteria incubated with [PI(4,5)P2] did not aggregate into microcolonies as quickly as [PI(3,4,5)P3] (data not shown). These results suggest that [PI(3,4,5)P3] stimulates microcolony formation.

To determine whether [PI(3,4,5)P3] associates with the aggregating bacteria, MS11 was incubated for 60 min with [PI(3,4,5)P3] convalently attached to fluorescent beads. Bacteria were visualized by Differential Interference Contrast microscopy, and the beads were visualized using the FITC channel (Fig. 6A). As bacteria moved along the surface, they aggregated, actively acquiring lipid-coated beads into the developing microcolonies. The diffuse fluorescence of the [PI(3,4,5)P3] beads in these images (Fig. 6A, upper panel) is resulting from diffraction of fluorescence emission by bacteria. The same FITC image viewed by Differential Interference Contrast revealed the presence of microcolonies at these sites (Fig. 6A, lower panel). As observed in the previous assay, bacteria exposed to mock-coated beads aggregated to a lesser extent than those exposed to [PI(3,4,5)P3]-coated beads, and their microcolonies were much smaller. Bacteria rarely incorporated mock-coated beads into their microcolonies, even though they came into physical contact with the beads (Fig. 6B).

Once a lipid-coated bead was 'engulfed' by a microcolony, it remained within the structure and moved with it. Time-lapsed video microscopy (see *Supplementary material*) revealed the microcolony-incorporated beads in constant motion resembling twitching behaviour. Mock-coated beads remained attached to the coverslip even if they had been touched by a passing microcolony. Taken together, these imaging studies demonstrate that host cell [PI(3,4,5)P3] enhances GC microcolony formation.

[PI(3,4,5)P3] upregulates pilT

GC twitching motility and pilus retraction require *pilT*. The effect of [PI(3,4,5)P3] on GC movement and microcolony formation led us to determine whether this phospholipid affected *pilT* expression. Wild-type MS11 was incubated for 2 h with soluble [PI(3,4,5)P3], [PI(4,5)P2], or vehicle alone, and the level of *pilT* message was determined by quantitative real-time polymerase chain reaction (PCR). Expression of *pilT* increased 1.8-fold (SD $\pm$ 0.2) in cultures incubated with [PI(4,5)P3]. This response is specific to [PI(3,4,5)P3], as neither vehicle nor [PI(4,5)P2] altered *pilT* expression. [PI(4,5)P2] differs from [PI(3,4,5)P3] by the absence of a phosphate group in the inositol ring. Thus, [PI(3,4,5)P3] not only affects motility behaviour, it also affects expression of a gene that is involved in twitching motility and pilus retraction.

Discussion

The *N. gonorrhoeae* type IV pilus modulates host cell functions during infection (Kallstrom *et al*., 1998; Merz and So, 2000; Lee *et al*., 2002). We tested the hypothesis that pilus retraction can also influence GC interactions with the epithelial cell. We presented evidence that GC activates the PI3-kinase/Akt signalling pathway in human epithelial cells, and that this activation requires, in part, a functional *pilT* (Fig. 1). The PI-3 kinase pathway plays a role in invasion, as wortmannin and LY294002 reduce invasion by 81.6% ($P = 0.005$) and 50.0% ($P = 0.001$) respectively (Fig. 2).

A number of bacterial pathogens use the PI-3 kinase pathway to trigger cytoskeleton remodelling and/or modulate phagocytic events that promote invasion (Ireton and Cossart, 1997; Coombes *et al*., 2002; Kwok *et al*., 2002). How these pathogens activate PI-3 kinase is not known. Non-piliated GC can activate PI-3 kinase through Opa binding of CEACAM-3 (Booth *et al*., 2003). Our study indicates that the GC type IV pilus can also activate this cascade.

Two different approaches show that [PI(3,4,5)P3], the direct product of activated PI-3 kinase, is exposed on the outer leaflet of the infected cell membrane. Although phosphoinositides are usually localized to the cytoplasmic leaflet of the eucaryotic plasma membrane, they and other lipid moieties can be translocated across the membrane bilayer and/or released into the medium (Daleke, 2003). Physiological levels of exogenous [PI(3,4,5)P3], but not [PI(3,4)P(2)], PI[(4,5)P(2)] or PI[(3)P], induce Ca^{2+} fluxes in T cells, implying that extracellular [PI(3,4,5)P3] has an important role in cellular communication (Hsu *et al*., 2000). That [PI(3,4,5)P3] is present on the outer face of the infected cell membrane, in close proximity to the attached microcolony, suggests that the colonizing bacteria may have access to this pool of lipids.

What might be the function(s) of [PI(3,4,5)P3] in GC–host cell interactions? *H. pylori, Chlamydia trachomatis* and *Campylobacter upsaliensis* bind host lipids with high affinity (Lingwood *et al*., 1992; Huesca *et al*., 1996; Sylvester *et al*., 1996; Busse *et al*., 1997; Barnett Foster *et al*., 1999), leading to the hypothesis that lipids promote bacterial attachment. In this model, [PI(3,4,5)P3] binding would strengthen physical contact between the bacterium and epithelial cell.

Alternatively, [PI(3,4,5)P3] may act as a chemoattractant, its accumulation at the site of infection creating a gradient that is recognized by the bacteria. Several studies support this hypothesis. A number of lipids affect bacterial twitching motility behaviour. Certain phosphoethanolamine (PE) species are chemoattractants for *M. xanthus*, stimulating type IV pilus-dependent social motility (Kearns and Shimkets, 2001). Others enhance the

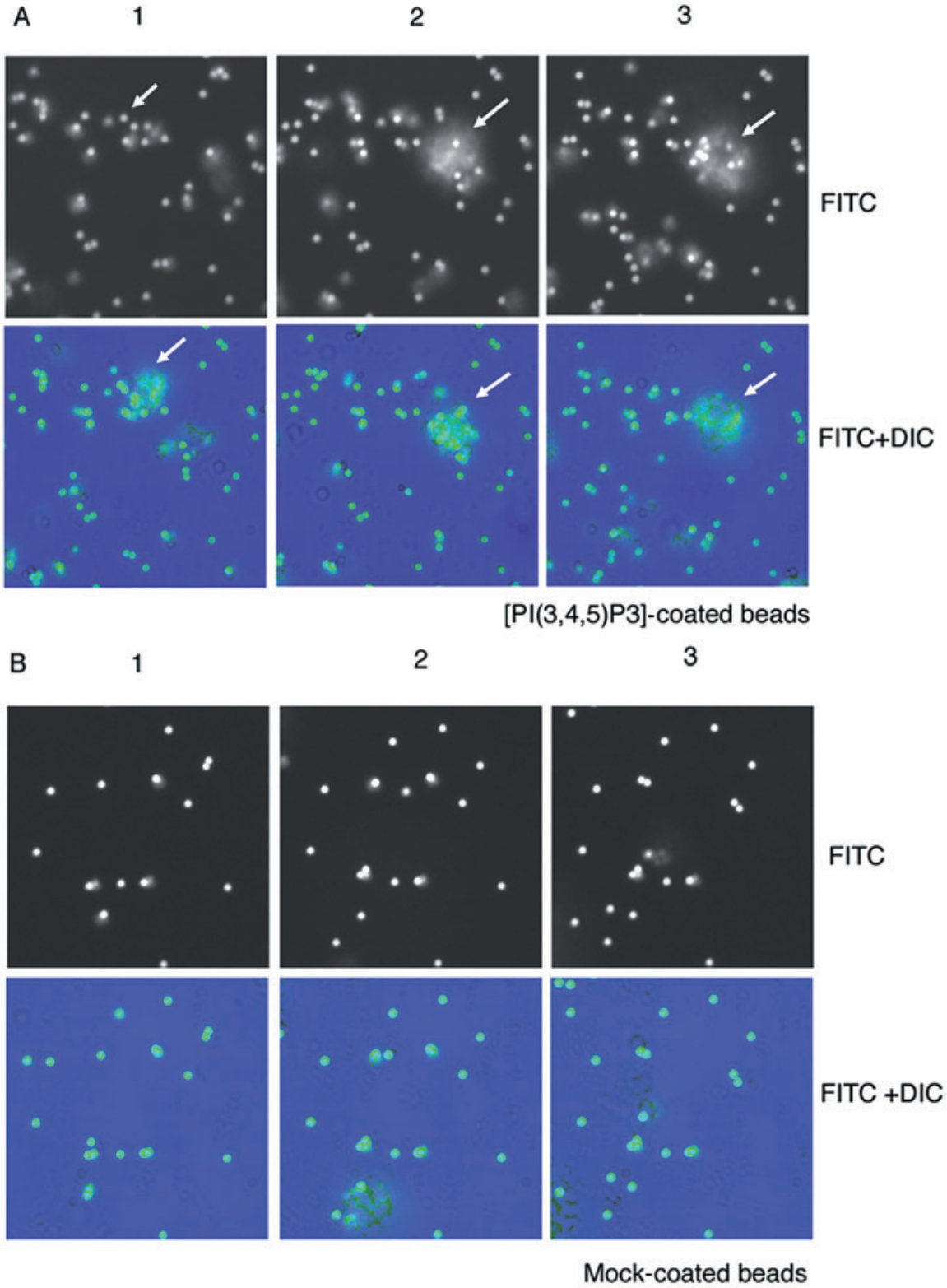

Fig. 6. Time-lapsed microscopy of wt MS11 in the presence of [PI(3,4,5)P3]-coated fluorescent beads.
A. MS11 bacteria were suspended on a glass slide and incubated with [PI(3,4,5)P3]-coated beads for 15 (column 1), 30 (column 2) and 60 (column 3) min. Images in the top row were obtained using the FITC channel to reveal bead position (also denoted by arrow). Images in the bottom row show overlays of the FITC and Differential Interence Constrast (DIC) images to reveal bacterial aggregates.
B. The same experiment performed by incubating MS11 with mock-coated fluorescent beads. Time-lapsed images were translated into Quicktime format using a Silicon Graphics workstation with accompanying API software (see video).

twitching velocity of *P. aeruginosa* type IV pili (Kearns and Shimkets, 1998). PE also induces aggregation of enteropathogenic and enterohaemorrhagic *E. coli* (Barnett Foster *et al*., 1999). Consistent with these findings, we observe that [PI(3,4,5)P3] affects GC aggregation/microcolony formation (Fig. 5) and upregulates transcription of *pilT*, the gene encoding the presumptive retraction motor. That [PI(4,5)P2] had no effect on *pilT* expression indicates the specificity of the latter response and lends further support for this hypothesis. PilT protein levels were not measured in this study. However, a 1.8-fold increase in the level of a transcript could result in a much higher-fold increase in its translated product.

As in the case for other bacteria, the details of phospholipids signalling between GC and the host cell remain to be defined. In light of the above observations, it is tempting to speculate that [PI(3,4,5)P3] alters the pilus retraction process, perhaps by increasing its rate of retraction, its force of retraction, or both. One direct consequence of increased *pilT* expression might be an increase in the number of retractile motors, which in turn would increase the overall rate of retraction.

Both models of [PI(3,4,5)P3] function require the translocation of this phospholipid across the plasma membrane. The molecular basis for this reaction is unclear, though precedents exist for the translocation of other lipids. A number of enzymes are known to translocate PE and PI (phosphatidylinositols) to the outer leaflet of the lipid bilayer (Daleke, 2003). Lipids can be externalized by stress (van Engeland *et al*., 1998) and by bacterial infection (Fujimoto *et al*., 1998; Gao and Abu Kwaik, 1999; Goth and Stephens, 2001; Hoffmann *et al*., 2001b), and the latter event is postulated to stimulate phagocytosis.

The membrane translocation of [PI(3,4,5)P3] and PS does not necessarily indicate that the infected cell is undergoing apoptosis. Indeed, there is evidence to suggest the opposite. *Chlamydia*-triggered translocation of PS correlates with anti-apoptotic effects in the cell (Greene *et al*., 2004). *Porphyromonas gingivalis* infection stimulates early translocation of PS while activating PI3K/Akt to promote host survival (Yilmaz *et al*., 2004). PS externalization and clustering on phagocyte membranes may serve to stimulate microbial engulfment (Fadok *et al*., 2000). Finally, recent studies in our lab indicate that pilus retraction activates cytoprotective cascades that override apoptosis signalling in infected cells (Howie *et al*., submitted).

Our study shows that communication of GC with the epithelial cell via the type IV pilus is bi-directional, involving an extended dialogue between bacterial and host components. This mode of bacteria-host cell communication has gained attention by the recent discovery that the eucaryotic hormones epinephrine and norepinephrine induce quorum sensing and regulate virulence gene expression among EHEC (Sperandio *et al*., 2003). Further studies should provide new insight into the role of interspecies signalling in bacterial pathogenesis.

Experimental procedures

Reagents, cell lines, bacterial strains and infections

Wortmannin, LY294002, soluble [PI(3,4,5)P3] and [PI(4,5)P2] were purchased from Calbiochem; TPA (Phorbol-12 Myristate-13–Acetate) from Cell Signaling Technologies. Antibodies were purchased from the following: PI-3 kinase p110 subunit and phospho-Akt from Cell Signaling Technologies; PS from Chemicon; phospho-adducin from Upstate Biotechnologies; ezrin from BD Transduction Laboratories; [PI(3,4,5)P3] from Echelon Biochemical; β-tubulin clone E7 from the Developmental Studies Hybridoma Bank; Alexa-488- and Alexa-572-labelled secondary antibodies from Molecular Probes. The PI-3 kinase detection ELISA kit was purchased from Echelon Biochemical.

A431 cells were maintained in DMEM with 10% heat-inactivated FBS at 37°C (Life Technologies) and 5% CO_2. GC wt strain MS11 (Segal *et al*., 1986) and an isogenic GC *pilT* mutant was used for infection experiments. The piliation and Opa status of all strains and inocula were monitored by microscopy observation of colony morphology, immunoblotting with antibodies directed against pilin (Virji *et al*., 1989) and Opa using the pan-Opa antibody 4B12 from M. Blake(Blake *et al*., 1995). The MS11 *pilT* null mutant was constructed by transforming chromosomal DNA from strain GT103 (N400 P+, Opa–, *pilT*::mTnErm) (Wolfgang *et al*., 1998b) into MS11 and selecting transformants for erythromycin resistance. *pilE* expression was confirmed by Western blotting and piliation was determined by immunofluorescence microscopy using a rabbit polyclonal antibody raised against total GC proteins. Loss of *pilT* function was determined by loss of competence for DNA transformation. One *pilT* candidate was selected and chromsomal DNA isolated and used to backcross (retransform) the same stock of MS11, with tests repeated. Transformation was used to transfer the isopropyl β-D-thiogalactopyranoside (IPTG)-inducible *pilT* gene in strain MW4 (Wolfgang *et al*., 1998b) into MS11 to yield the MS11 inducible *pilT* mutant used in this study. Piliation and Opa phenotypes were monitored by colony morphology.

Adhesion assay

A431 cells were grown to 80% confluency in 12 well Plate 24 h prior to infection. Adhesion was measured as described previously (Shaw and Falkow, 1988; Waldbeser *et al*., 1994). Cells were washed three times with serum-free DMEM prior to infection and incubated for 1 h in serum-free medium containing LY294002 (50 μM), wortmannin (10 nM), or medium alone. Bacteria were then added to the cultures at a multiplicity of infection (moi) of 50, and the cultures were incubated for 3 h in the presence of inhibitor. Supernatants were collected and saved for plating. Infected cultures were washed five times in PBS and the washes also saved and plated (see below). Washed cells were then lysed in liquid GCB medium with saponin (0.5%, wt/vol). Serial dilutions of the lysates were plated on supplemented GCB agar, the plates were grown for 48 h at 37°C, 5% CO_2, and colony-forming units (cfu) were counted. Adhesion index

was measured as the number of cell-associated bacteria divided by the total number of bacteria in the well at the end of the infection.

Gentamicin protection assay

Gentamicin protection assays (Shaw and Falkow, 1988) were performed as described previously (Waldbeser *et al.*, 1994). A431 cells were grown to 80% confluency in 12 well Plate 24 h prior to infection. Cells were washed three times with serum-free DMEM prior to infection and incubated in serum-free medium with LY294002 or wortmannin as described above. Cells were infected for 6 h with MS11 at an moi of 50. Cells were then incubated with Gentamicin (100 μg ml^{-1}) for 1 h at 37°C to kill extracellular and attached bacteria. After washing five times in PBS to remove non-adherent bacteria, the cells were lysed. The lysates were collected in GCB plus saponin (0.5%, wt/vol) and serially diluted and spread onto supplemented GCB plates. The plates were incubated for 48 h at 37°C, 5% CO_2, and colony forming units were determined. Invasion index is calculated as the number of Gentamicin-resistant bacteria divided by the number of cell-associated (adhered and invaded) bacteria in the well at the end of the infection.

Akt kinase assay

A431 cells were infected with GC wt strain MS11 and an isogenic GC *pilT* mutant at an moi of 50 for various lengths of time. Akt was immunoprecipitated from infected cells using an Akt kinase assay kit (Cell Signaling Technology). Akt activity was assayed using an Akt kinase assay kit (Cell Signaling Technology). Akt activity was measured by using a phospho-GSK-3α/β antibody to detect kinase activity of immunoprecipitated Akt after incubation with a GSK fusion peptide. Phospho-Akt antibodies were used to confirm levels of Akt activity. Polyclonal antibodies to Akt were used to confirm total levels of Akt in lysates.

Immunofluorescence microscopy

A431 cells were grown on coverslips to 30–50% confluence and infected for 3 h with MS11 at an moi of 100. Coverslips were washed three times in PBS, fixed for 20 min at room temperature in 4% paraformaldehyde, and blocked for 1 h in isotonic PBS containing normal goat serum (3%, v/v) and saponin (0.02%, wt/vol). To determine the presence of [PI(3,4,5)P3] on the outer leaflet of the membrane, saponin was omitted from all blocking and incubation steps. Primary antibody was diluted as specified above in blocking buffer, added to samples, and incubated overnight at 4°C in a moist chamber. The coverslips were rinsed in PBS and incubated with an Alexa conjugated secondary antibody diluted 1:500 in blocking buffer for 1 h at 25°C. Samples to visualize outer membrane proteins and phospholipids were all incubated at 4°C for all steps. The cells were also incubated with the DNA stain DAPI at 1:1000 for 10 min at 25°C to visualize the bacteria and nuclei. Samples were rinsed extensively in PBS before mounting in Fluoromount-G (Fisher Scientific). Negative control samples were processed identically except for the omission of primary antibodies. Optical sections in the *z*-axis plane were obtained with a Deltavision Restoration Microscope (Applied Precision Instruments, Inc.) fitted with a Nikon 60x oil immersion objective, and the images were processed at a Silicon Graphics workstation with accompanying API software. The images were subsequently exported to Adobe Photoshop and Adobe Illustrator for manuscript preparation.

PI-3 kinase ELISA

ELISA to determine levels of [PI(3,4,5)P3] in A431 cell supernatants was performed using a PI-3 kinase assay kit (Echelon BioSciences) per manufacturer's instructions except the supernatants from infected and uninfected A431 cells were incubated with the [PI(3,4,5)P3] detection reagent at 4°C for 18 h. Cells were infected with GC wt strain MS11 at an moi of 50 for 3 h, and the supernatants collected for analysis. Control wells containing either uninfected cells or cells incubated with bacteria alone were used to eliminate cross-reactivity. The reaction mixtures were then transferred to the detection plate and all other steps performed as indicated. [PI(3,4,5)P3] levels were detected using a MicroMax plate reader using absorbance at 450 nm. Levels of [PI(3,4,5)P3] were quantified by comparing values from wells containing supernatants from cells to the values in a standard curve run concomitantly with test wells.

Phospho-adducin assay

Adducin phosphorylation following GC infection was determined using a phospho-adducin (Ser 724) antibody (Upstate Biotechnologies). Monoclonal antibodies to β-tubulin were used to normalize protein levels in lysate samples. As a positive control, uninfected cells were treated for 1 h with 0.2 μM TPA (Phorbol-12 Myristate-13–Acetate).

Bacterial aggregation (microcolony formation) assay

Wide-type MS11 bacteria were diluted to approximately 5×10^8 cfu ml^{-1} in supplemented GCB medium in a total volume of 1 ml. 10 μg of soluble [PI(3,4,5)P3] or [PI(4,5)P2] (Calbiochem) was added at a concentration of 1μg/μl and the samples vortexed for 1 min. 100 μl of the culture was added to a coverdish (Costar) and bacterial aggregation was monitored in real time at room temperature by Differential Interference Contrast microscopy using the Deltavision Restoration Microscope (API).

[PI(3,4,5)P3] bead aggregation assays

1.0 μm yellow-green fluorescent polystyrene beads (Fluospheres, Molecular probes) were covalently coupled with soluble [PI(3,4,5)P3] (Calbiochem) using water-soluble caboiimide (EDAC) as recommended by the supplier. The beads were washed thoroughly in PBS and adsorbed onto a clean coverslip dish in the presence of PBS. BSA (bovine serum albumin) was used to coat mock beads for controls. GC cultures were added as stated for aggregation assays. Differential Interference Contrast and fluorescence microscopy was used to visualize aggregating bacteria and beads respectively. Time-lapsed movies were produced in Quicktime format using a SiliconGraphics workstation with accompanying API software.

RNA extraction and real-time RT-PCR assays

Bacterial RNA was extracted from MS11 using the RNAeasy kit (Qiagen) per manufacturer's instructions. Briefly, wt MS11 was diluted in supplemented GCB medium and incubated with 20 μg of [PI(3,4,5)P3], [PI(4,5)P2] or a vehicle control for 2 h before collection. Cells were lysed in lysozyme (0.4 $\mu g\ \mu^{-1}$l wt/vol) containing Tris-EDTA buffer. DNA contamination was removed by treatment with DNA-free (Ambion) and samples were quantified by spectrophotometric analysis (Beckman DU 600). Complementary DNA was generated using the iScript cDNA Synthesis Kit (Bio-Rad) as recommended by the manufacturer. Oligonucleotides complementary to *pilT* were designed using the primer express software (PE Applied biosystems) to obtain amplicons of the same size. Oligonucleotides to *pilT (*pilTin.630, 5′-GTC GACCGTATCGTGGACGTATT-3′; pilTout.730, 5′-TTCAGCAG GTTTTGGGAGATGAC-3′) were purchased from Invitrogen.

Real-time PCR using SYBR GREEN PCR Master Mix (Applied Biosystems) was carried out on the ABI Prism 7000 Sequence Detector System (Applied Biosystems). Amplification plots were analysed with the ABI Prism SDS Software package (Version 1.0) and the data were processed using TaqMan Turbocrunch (96) v3. Relative quantification of gene expression was performed by the comparative Ct (threshold cycle) method according to the manufacturer's instructions and as published (Schmittgen *et al*., 2000). The parameter Ct is defined as the cycle number at which fluorescence passes the fixed threshold. Two independent real-time reverse transcription polymerase chain reaction (RT-PCR) experiments were performed. Dilutions of the reverse transcription product from each experiment were loaded in triplicate for each oligonucleotide couple in all experiments.

Acknowledgements

We thank Michael Sheetz at Columbia University for critical comments. We thank Patricia Ayala, Heather Howie, Robert Bonnah, Jason Larson and George Niemann for their expert technical assistance; all of the members of the So Laboratory for helpful comments on the manuscript; and J. Scott Wilbur and Chris Langford for their help in preparing the manuscript. This work was funded by NIH Grants AI32493 and AI4997301 to M. So.

References

Ayala, B.P., Vasquez, B., Clary, S., Tainer, J.A., Rodland, K., and So, M. (2001) The pilus-induced Ca^{2+} flux triggers lysosome exocytosis and increases the amount of Lamp1 accessible to Neisseria IgA1 protease. *Cell Microbiol* **3:** 265–275.

Barnett Foster, D., Philpott, D., Abul-Milh, M., Huesca, M., Sherman, P.M., and Lingwood, C.A. (1999) Phosphatidylethanolamine recognition promotes enteropathogenic *E. coli* and enterohemorrhagic *E. coli* host cell attachment. *Microb Pathog* **27:** 289–301.

Berridge, M.J., Bootman, M.D., and Roderick, H.L. (2003) Calcium signalling: dynamics, homeostasis and remodelling. *Nat Rev Mol Cell Biol* **4:** 517–529.

Bhaya, D., Takahashi, A., and Grossman, A.R. (2001) Light regulation of type IV pilus-dependent motility by chemosensor-like elements in Synechocystis PCC6803. *Proc Natl Acad Sci USA* **98:** 7540–7545.

Blake, M.S., Blake, C.M., Apicella, M.A., and Mandrell, R.E. (1995) Gonococcal opacity: lectin-like interactions between Opa proteins and lipooligosaccharide. *Infect Immun* **63:** 1434–1439.

Booth, J.W., Telio, D., Liao, E.H., McCaw, S.E., Matsuo, T., Grinstein, S., and Gray-Owen, S.D. (2003) Phosphatidylinositol 3-kinases in carcinoembryonic antigen-related cellular adhesion molecule-mediated internalization of *Neisseria gonorrhoeae*. *J Biol Chem* **278:** 14037–14045.

Busse, J., Hartmann, E., and Lingwood, C.A. (1997) Receptor affinity purification of a lipid-binding adhesin from Haemophilus influenzae. *J Infect Dis* **175:** 77–83.

Cantley, L.C. (2002) The phosphoinositide 3-kinase pathway. *Science* **296:** 1655–1657.

Chapline, C., Ramsay, K., Klauck, T., and Jaken, S. (1993) Interaction cloning of protein kinase C substrates. *J Biol Chem* **268:** 6858–6861.

Comolli, J.C., Waite, L.L., Mostov, K.E., and Engel, J.N. (1999) Pili binding to asialo-GM1 on epithelial cells can mediate cytotoxicity or bacterial internalization by *Pseudomonas aeruginosa*. *Infect Immun* **67:** 3207–3214.

Coombes, B.K., Johnson, D.L., and Mahony, J.B. (2002) Strategic targeting of essential host–pathogen interactions in chlamydial disease. *Curr Drug Targets Infect Disord* **2:** 201–216.

Daleke, D.L. (2003) Regulation of transbilayer plasma membrane phospholipid asymmetry. *J Lipid Res* **44:** 233–242.

Dong, L., Chapline, C., Mousseau, B., Fowler, L., Ramsay, K., Stevens, J.L., and Jaken, S. (1995) 35H, a sequence isolated as a protein kinase C binding protein, is a novel member of the adducin family. *J Biol Chem* **270:** 25534–25540.

van Engeland, M., Nieland, L.J., Ramaekers, F.C., Schutte, B., and Reutelingsperger, C.P. (1998) Annexin V-affinity assay: a review on an apoptosis detection system based on phosphatidylserine exposure. *Cytometry* **31:** 1–9.

Fadok, V.A., Bratton, D.L., Rose, D.M., Pearson, A., Ezekewitz, R.A., and Henson, P.M. (2000) A receptor for phosphatidylserine-specific clearance of apoptotic cells. *Nature* **405:** 85–90.

Fujimoto, I., Takizawa, T., Ohba, Y., and Nakanishi, Y. (1998) Co-expression of Fas and Fas-ligand on the surface of influenza virus-infected cells. *Cell Death Differ* **5:** 426–431.

Gao, L.Y., and Abu Kwaik, Y. (1999) Apoptosis in macrophages and alveolar epithelial cells during early stages of infection by Legionella pneumophila and its role in cytopathogenicity. *Infect Immun* **67:** 862–870.

Gomez-Duarte, O.G., Dehio, M., Guzman, C.A., Chhatwal, G.S., Dehio, C., and Meyer, T.F. (1997) Binding of vitronectin to opa-expressing *Neisseria gonorrhoeae* mediates invasion of HeLa cells. *Infect Immun* **65:** 3857–3866.

Goth, S.R., and Stephens, R.S. (2001) Rapid, transient phosphatidylserine externalization induced in host cells by infection with Chlamydia spp. *Infect Immun* **69:** 1109–1119.

Greene, W., Xiao, Y., Huang, Y., McClarty, G., and Zhong, G. (2004) Chlamydia-infected cells continue to undergo mitosis and resist induction of apoptosis. *Infect Immun* **72:** 451–460.

Herdendorf, T.J., McCaslin, D.R., and Forest, K.T. (2002) Aquifex aeolicus PilT, homologue of a surface motility protein, is a thermostable oligomeric NTPase. *J Bacteriol* **184:** 6465–6471.

Hoffmann, I., Eugene, E., Nassif, X., Couraud, P.O., and

Bourdoulous, S. (2001a) Activation of ErbB2 receptor tyrosine kinase supports invasion of endothelial cells by *Neisseria meningitidis*. *J Cell Biol* **155:** 133–143.

Hoffmann, P.R., deCathelineau, A.M., Ogden, C.A., Leverrier, Y., Bratton, D.L., Daleke, D.L., *et al.* (2001b) Phosphatidylserine (PS) induces PS receptor-mediated macropinocytosis and promotes clearance of apoptotic cells. *J Cell Biol* **155:** 649–659.

Hsu, A.L., Ching, T.T., Sen, G., Wang, D.S., Bondada, S., Authi, K.S., and Chen, C.S. (2000) Novel function of phosphoinositide 3-kinase in T cell Ca2+ signaling. A phosphatidylinositol 3,4,5-trisphosphate-mediated Ca2+ entry mechanism. *J Biol Chem* **275:** 16242–16250.

Huesca, M., Borgia, S., Hoffman, P., and Lingwood, C.A. (1996) Acidic pH changes receptor binding specificity of *Helicobacter pylori*: a binary adhesion model in which surface heat shock (stress) proteins mediate sulfatide recognition in gastric colonization. *Infect Immun* **64:** 2643–2648.

Ireton, K., and Cossart, P. (1997) Host–pathogen interactions during entry and actin-based movement of *Listeria monocytogenes*. *Annu Rev Genet* **31:** 113–138.

Kallstrom, H., Liszewski, M.K., Atkinson, J.P., and Jonsson, A.B. (1997) Membrane cofactor protein (MCP or CD46) is a cellular pilus receptor for pathogenic Neisseria. *Mol Microbiol* **25:** 639–647.

Kallstrom, H., Islam, M.S., Berggren, P.O., and Jonsson, A.B. (1998) Cell signaling by the type IV pili of pathogenic Neisseria. *J Biol Chem* **273:** 21777–21782.

Kearns, D.B., and Shimkets, L.J. (1998) Chemotaxis in a gliding bacterium. *Proc Natl Acad Sci USA* **95:** 11957–11962.

Kearns, D.B., and Shimkets, L.J. (2001) Lipid chemotaxis and signal transduction in *Myxococcus xanthus*. *Trends Microbiol* **9:** 126–129.

Kwok, T., Backert, S., Schwarz, H., Berger, J., and Meyer, T.F. (2002) Specific entry of *Helicobacter pylori* into cultured gastric epithelial cells via a zipper-like mechanism. *Infect Immun* **70:** 2108–2120.

Lee, S.W., Bonnah, R.A., Higashi, D.L., Atkinson, J.P., Milgram, S.L., and So, M. (2002) CD46 is phosphorylated at tyrosine 354 upon infection of epithelial cells by *Neisseria gonorrhoeae*. *J Cell Biol* **156:** 951–957.

Lin, L., Ayala, P., Larson, J., Mulks, M., Fukuda, M., Carlsson, S.R., *et al.* (1997) The Neisseria type 2 IgA1 protease cleaves LAMP1 and promotes survival of bacteria within epithelial cells. *Mol Microbiol* **24:** 1083–1094.

Lingwood, C.A., Huesca, M., and Kuksis, A. (1992) The glycerolipid receptor for *Helicobacter pylori* (and exoenzyme S) is phosphatidylethanolamine. *Infect Immun* **60:** 2470–2474.

Maier, B., Potter, L., So, M., Long, C.D., Seifert, H.S., and Sheetz, M.P. (2002) Single pilus motor forces exceed 100 pN. *Proc Natl Acad Sci USA* **99:** 16012–16017.

Makino, S., van Putten, J.P., and Meyer, T.F. (1991) Phase variation of the opacity outer membrane protein controls invasion by *Neisseria gonorrhoeae* into human epithelial cells. *EMBO J* **10:** 1307–1315.

Merz, A.J., and So, M. (2000a) Interactions of pathogenic neisseriae with epithelial cell membranes. *Annu Rev Cell Dev Biol* **16:** 423–457.

Merz, A.J., Enns, C.A., and So, M. (1999) Type IV pili of pathogenic neisseriae elicit cortical plaque formation in epithelial cells. *Mol Microbiol* **32:** 1316–1332.

Merz, A.J., So, M., and Sheetz, M.P. (2000b) Pilus retraction powers bacterial twitching motility. *Nature* **407:** 98–102.

Miao, H., Yuan, S., Wang, Y., Tsygankov, A., Chien, S. (2002) Role of Cbl in shear-activation of PI 3-kinase and JNK in endothelial cells. *Biochem Biophys Res Commun* **292:** 892–899.

Raucher, D., Stauffer, T., Chen, W., Shen, K., Guo, S., York, J.D., *et al.* (2000) Phosphatidylinositol 4,5-bisphosphate functions as a second messenger that regulates cytoskeleton-plasma membrane adhesion [In Process Citation]. *Cell* **100:** 221–228.

Schmittgen, T.D., Zakrajsek, B.A., Mills, A.G., Gorn, V., Singer, M.J., and Reed, M.W. (2000) Quantitative reverse transcription-polymerase chain reaction to study mRNA decay: comparison of endpoint and real-time methods. *Anal Biochem* **285:** 194–204.

Segal, E., Hagblom, P., Seifert, H.S., and So, M. (1986) Antigenic variation of gonococcal pilus involves assembly of separated silent gene segments. *Proc Natl Acad Sci USA* **83:** 2177–2181.

Shaw, J.H., and Falkow, S. (1988) Model for invasion of human tissue culture cells by *Neisseria gonnorrhoeae*. *Infect Immun* **56:** 1625–1632.

Skerker, J.M., and Berg, H.C. (2001) Direct observation of extension and retraction of type IV pili. *Proc Natl Acad Sci USA* **98:** 6901–6904.

Sperandio, V., Torres, A.G., Jarvis, B., Nataro, J.P., and Kaper, J.B. (2003) Bacteria-host communication: the language of hormones. *Proc Natl Acad Sci USA* **100:** 8951–8956.

Strom, M.S., and Lory, S. (1993) Structure-function and biogenesis of the type IV pili. *Annu Rev Microbiol* **47:** 565–596.

Sylvester, F.A., Philpott, D., Gold, B., Lastovica, A., and Forstner, J.F. (1996) Adherence to lipids and intestinal mucin by a recently recognized human pathogen, *Campylobacter upsaliensis*. *Infect Immun* **64:** 4060–4066.

Virji, M., Heckels, J.E., Potts, W.J., Hart, C.A., and Saunders, J.R. (1989) Identification of epitopes recognized by monoclonal antibodies SM1 and SM2 which react with all pili of *Neisseria gonorrhoeae* but which differentiate between two structural classes of pili expressed by *Neisseria meningitidis* and the distribution of their encoding sequences in the genomes of Neisseria spp. *J Gen Microbiol* **135:** 3239–3251.

Waldbeser, L.S., Ajioka, R.S., Merz, A.J., Puaoi, D., Lin, L., Thomas, M., and So, M. (1994) The opaH locus of *Neisseria gonorrhoeae* MS11A is involved in epithelial cell invasion. *Mol Microbiol* **13:** 919–928.

Wang, N., Butler, J.P., and Ingber, D.E. (1993) Mechanotransduction across the cell surface and through the cytoskeleton. [See comments]. *Science* **260:** 1124–1127.

Wolfgang, M., Park, H.S., Hayes, S.F., van Putten, J.P., and Koomey, M. (1998a) Suppression of an absolute defect in type IV pilus biogenesis by loss-of-function mutations in *pilT*, a twitching motility gene in *Neisseria gonorrhoeae*. *Proc Natl Acad Sci USA* **95:** 14973–14978.

Wolfgang, M., Lauer, P., Park, H.S., Brossay, L., Hebert, J., and Koomey, M. (1998b) PilT mutations lead to simultaneous defects in competence for natural transformation and twitching motility in piliated *Neisseria gonorrhoeae*. *Mol Microbiol* **29:** 321–330.

Wu, S.S., Wu, J., and Kaiser, D. (1997) The *Myxococcus*

xanthus pilT locus is required for social gliding motility although pili are still produced. *Mol Microbiol* **23:** 109–121.

Yilmaz, O., Jungas, T., Verbeke, P., and Ojcius, D.M. (2004) Activation of the phosphatidylinositol 3-kinase/Akt pathway contributes to survival of primary epithelial cells infected with the periodontal pathogen *Porphyromonas gingivalis*. *Infect Immun* **72:** 3743–3751.

Supplementary material

The following material is available for this article online:

Videos S1 and S2. Time-lapsed microscopy of wt MS11 in the presence of [PI(3,4,5)P3]- or mock-coated fluorescent beads.